STU SvF
SLOVAK UNIVERSITY OF TECHNOLOGY IN BRATISLAVA
FACULTY OF CIVIL ENGINEERING

Slovak Journal of Civil Engineering

Vol. 33, 2025, No. 4, 21 – 30
DOI: 10.2478/sjce-2025-0024

PROJECTING THE FUTURE BIOCLIMATIC ENVIRONMENT OF BRATISLAVA: A UTCI-BASED ANALYSIS UNDER REPRESENTATIVE CONCENTRATION PATHWAY SCENARIOS

Tomáš HAKSZER[1*], Peter HANULIAK[1]

Abstract

This article deals with a future projection of the bioclimatic environment in Bratislava, Slovakia, under ongoing climate change. Using Meteonorm-generated climate data of up to 2100, this research paper presents calculations of the Universal Thermal Climate Index (UTCI) for three Representative Concentration Pathway scenarios, i.e., RCP2.6, RCP4.5, and RCP8.5. The analysis of hourly UTCI values quantifies projected shifts in human thermal stress, with the linear regression revealing strong temporal trends ($R^2 > 0.97$, $p < 0.05$). The main conclusions point to a significant transformation of the city's climate. Under the high-emissions RCP8.5 scenario, the annual duration of strong heat stress (UTCI ≥ +32°C) is projected to surge from a contemporary baseline of 66 hours to 936 by 2100. Concurrently, annual cold stress (UTCI ≤ 0°C) hours are expected to decrease from 851 to 312. The high degree of variability in the RCP8.5 scenario (CV = 61%) indicates increasing uncertainty in extreme conditions. This dual shift confirms the city's thermal character will be fundamentally altered, thereby leading to prolonged, stressful summers and milder winters. These findings provide a quantitative evidence base for local policymakers to develop urgent public health and urban adaptation strategies and can further support architects and civil engineers in the future design of resilient buildings through simulation-based solutions.

Address

[1] Faculty of Civil Engineering, Slovak University of Technology, Radlinského 11, 810 05, Bratislava, Slovakia

[*] ***Corresponding author:*** tomas.hakszer@stuba.sk

Key words

- Climate change,,
- Universal Thermal Climate Index,
- Thermal comfort,
- Representative Concentration Pathways,
- Bratislava.

1 INTRODUCTION

Projecting the future climate involves creating plausible descriptions of how the Earth's climate system might evolve in response to various anthropogenic and natural influences. The aim is not to provide exact predictions, but rather to explore the potential consequences of different human actions and policy choices (for example, urban planning and environmental policies). In climate change research, these descriptions are known as scenarios, i.e., simplified, internally consistent tools used to investigate potential outcomes and inform decision-making (Moss et al. 2010; Wayne 2013; Bjørnæs 2022).

1.1 Representative Concentration Pathways Scenarios as a Basis for Climate Projections

To provide a standardized framework for this research, the Intergovernmental Panel on Climate Change (IPCC) developed the Representative Concentration Pathways (RCPs) for its Fifth Assessment Report (IPCC 2014). The RCPs are the result of a multi-year collaboration between integrated assessment modelers, climate modelers, and emission inventory experts who combined historical data with future projections (Moss et al. 2010; Wayne 2013; Bjørnæs 2022; Van Vuuren et al. 2011; Meinshausen et al. 2011).

Each scenario is defined by a specific pathway of greenhouse gas concentrations, aerosols, and land-use changes, and by its corresponding total radiative forcing level for the year 2100. Radiative forcing is a metric that quantifies the change in the Earth-atmosphere energy balance; it is measured in W/m2 relative to a pre-industrial baseline. The term "pathway" emphasizes that the trajectory of emissions over time is as critical as the final stabilization level. Furthermore, each RCP is considered representative because it exemplifies one of many possible scenarios that could lead to the same radiative forcing characteristics (Moss et al. 2010; Wayne 2013; Bjørnæs 2022; Van Vuuren et al. 2011; Meinshausen et al. 2011).

Although climate scenarios are primarily developed within the domain of climate science, their relevance extends directly to architecture and building engineering. Anticipated changes in thermal stress, seasonal temperature patterns, and extreme events provide essential inputs for building performance simulations and urban design strategies. Integrating these data into practice allows architects and engineers to design climate-responsive buildings and resilient urban environments that safeguard occupant comfort and health under evolving climatic conditions (Zhai & Helman 2019, Niknia & Ghiai 2025).

This study focuses on three specific RCPs, which span a range from strong mitigation to high emissions; their key characteristics are summarized in Table 1 (Moss et al. 2010; Wayne 2013):

- RCP2.6 (Low Emissions/Peak and Decline): This is the most optimistic scenario and is consistent with a future involving declining oil use, low energy intensity, a global population peaking around 9 billion, increased use of croplands for bio-energy production, and stringent climate policies,

- RCP4.5 (Intermediate Emissions/Stabilization): This scenario represents a future where climate policies lead to a stabilization of radiative forcing; it is consistent with a future involving lower energy intensity, strong reforestation programs, decreasing use of croplands and grasslands, and stringent climate policies.

- RCP8.5 (High Emissions/Rising): This scenario represents a high-emissions future, which is often considered a business-as-usual or baseline scenario with no significant global climate mitigation policies. It is consistent with futures characterized by high population growth (e.g., 12 billion by 2100), a lower rate of technological development, heavy reliance on fossil fuels (especially coal), high energy intensity, and no implementation of widespread climate policies.

Niknia and Ghiai (2025) conducted a comprehensive simulation-based study utilising RCPs to predict the energy performance of office buildings across all U.S. climate zones under future climate conditions. They specifically employed RCP 4.5 to represent a moderate emissions scenario and RCP 8.5 to indicate a high-emissions future to project climate data for 2050 and 2080. The main results revealed significant shifts in energy demands. Quantitatively, their simulations showed that small office buildings may see a slight decrease in energy use intensity by about 2.5% under RCP 8.5 by 2080, whereas mid-sized and large offices could increase energy use by 12.5% and 7.4%. Offices in hot and humid regions could reach up to 21.2%. Across all the building types in the study, warmer regions consistently faced rising cooling energy requirements, while colder areas experienced decreases due to milder winters, which often led to net energy reductions in those regions.

1.2 Bioclimatic Marker for Climate Impact Studies

To quantitatively capture the interaction between climatic conditions and human thermal perception, this study applies a robust bioclimatic marker widely used in climate and health research. The key metric of this study is the Universal Thermal Climate Index (UTCI). The UTCI is a bioclimatic index that assesses the human physiological response to an outdoor thermal environment. It functions as an equivalent temperature and integrates the combined effects of air temperature, humidity, wind speed, and short-wave and long-wave radiation. For any given set of these atmospheric conditions, the UTCI value is the air temperature of a standardized reference environment that would provoke the exact same response from a human thermo-regulatory model. Expressing this complex thermal load as a simple temperature value allows the UTCI to be interpreted intuitively on a familiar scale in degrees Celsius (°C) (Bröde et al. 2011; 2012; 2010; Di Napoli et al. 2018).

Tab. 1 *Comparative Overview of RCP2.6, RCP4.5 and RCP8.5.*

Name	RCP2.6	RCP4.5	RCP8.5
Pathway Description	Peak and decline	Stabilization without overshoot	Rising
Radiative Forcing in 2100 (W/m^2)	2.6 (peak ~3.0 mid-century)	4.5 (stabilizing after 2100)	>8.5 (continuing to rise)
Approx. CO_2 Conc. in 2100 (ppm)	~421-490	~538-650	>900
Median Temp. Anomaly by 2100 (°C vs. pre-industrial)	~1.5	~2.4	~4.9
General Emissions Trajectory	Strong, early and sustained mitigation; CO_2 emissions negative by 2100	Moderate mitigation, CO_2 emissions peak around 2040, then decline	Continued high emissions; no climate policy
Key Socio-economic Assumptions	Lower population growth (peak ~9 billion), low energy intensity, high share of renewables, strong climate policies	Medium population growth, energy intensity improvements, some climate policies, reforestation	High population growth (~12 billion), high energy intensity, heavy fossil fuel reliance, slow technological change, no climate policy

The development of UTCI was a significant collaborative effort; it was initiated by Commission 6 of the International Society of Biometeorology (ISB) and strongly supported by the European Cooperation in Science and Technical Development Action 730 (Bröde et al. 2013; Nassiri et al. 2017; Pecelj et al. 2020; Jendritzky et al. 2002). The development of UTCI was successfully concluded in 2009 (Błażejczyk et al. 2013; Holmér et al. 2012). The UTCI represents the most advanced and comprehensive bioclimatic index currently available, although simpler and widely applied alternatives include the Heat Index (HI), Wet Bulb Globe Temperature (WBGT), Physiologically Equivalent Temperature (PET), and Predicted Mean Vote (PMV) (Črepinšek et al. 2023).

1.3 Physiological Basis of UTCI

The calculation of the UTCI is fundamentally based on the Fiala model, a sophisticated multi-node simulation of human thermo-regulation (Błażejczyk et al. 2013). The model's passive system represents an average person (body weight of 73.5 kg and Dubois-area of 1.86 m²) with 12 body elements and 187 tissue nodes to simulate heat and mass transfer. Its active system then predicts crucial thermos-regulatory actions, such as changes in skin blood flow, shivering thermogenesis, and sweat excretion (Błażejczyk et al. 2013). This core physiological model is coupled with an adaptive clothing model that accounts for behavioral realism by adjusting for the insulation effects of clothing based on the ambient temperature (0.4 - 2.6 clo), its distribution across the body, and the reduction in thermal resistance caused by wind and movement (Bröde et al. 2013). For the purpose of standardization, the final UTCI value is expressed as an equivalent temperature relative to a specific reference activity and environment. This reference assumes a person walking at 4 km/h (metabolic rate of 135 W/m²/2.3 MET) in an environment where the mean radiant temperature equals the air temperature, with a wind speed of 0.5 m/s (at 10 m height) and a specified reference humidity (Bröde et al. 2013). The UTCI is represented by the following equation (Bröde et al. 2012):

$$UTCI = Ta + \text{Offset}(Ta, Tmrt, Va, Td) = \text{f}(Ta, Tmr, Va, Td) \quad (1)$$

$$Tmrt = \left[\frac{Rprim + 0{,}5Lg + 0{,}5La}{5.39\text{x}10^{-8}} + (273 + t)^4\right]^{1/4} - 273 \quad (2)$$

$$L_g = 5.5\text{x}10^{-8}\left(273 + T_g\right)^4 \quad (3)$$

$$L_a = 5.5\text{x}10^{-8}(273 + T_a)^4 \quad (4)$$

$$Va = \sqrt{Vu^2 + Vv^2} \quad (5)$$

Where:
- L_a - Long-wave radiation flux density from the atmosphere (W/m²),
- L_g - Long-wave radiation flux density from the ground (W/m²),
- R_{prim} - Solar radiation absorbed by an unclothed person,
- T_a - 2-meter air temperature (°C),
- T_d - Dew point temperature (°C),
- T_g - Ground surface temperature (°C),
- T_{mrt} - Mean radiant temperature (°C),
- V_a - Wind speed (m/s),
- V_u - 10-meter U-component of wind speed (east- west),
- V_v - 10-meter V-component of wind speed (north- south).

This makes UTCI thermos-physiologically significant across the entire range of heat exchange conditions and ensures its validity in all climates, seasons, and spatial and temporal scales (Bröde et al. 2012; Pecelj et al. 2020; Błażejczyk et al. 2013; Črepinšek et al. 2023).

UTCI values are categorized into ten distinct thermal stress levels, ranging from extreme cold stress to extreme heat stress; the values for the individual categories are shown in Table 2 (Błażejczyk et al. 2013). Under moderate heat stress, the body initiates thermos-regulatory responses, including the onset of sweating within 30 minutes and a steep increase in the moisture of the skin. As conditions intensify to strong heat stress, the average sweat rate exceeds 200 g/h, and an increase in core body temperature is observed over a 120-minute period. With very strong heat stress, the core-to-skin temperature gradient diminishes to less than 1 K, and the core body temperature rises within the first 30 minutes. The most severe category, i.e., extreme heat stress, is characterized by a rapid increase in the core body temperature's time gradient, a sharp decline in total net heat loss, and a profuse average sweat rate greater than 650 g/h (Błażejczyk et al. 2013).

The "no thermal stress" category represents a state of thermal equilibrium, where the core body temperature's time gradient plateaus. Conversely, the onset of slight cold stress is marked by a noticeable drop in temperature of the skin on the hand, which indicates peripheral vasoconstriction. Under moderate cold stress, vasoconstriction intensifies; the core body temperature time gradient becomes negative; and the temperature of the skin of the face drops below 15°C, which may induce pain. Strong cold stress leads to a further decrease in the core body temperature and causes the skin temperature of the face to fall below 7°C, thereby resulting in numbness. At the very strong cold stress level, shivering occurs; the decline in core body temperature accelerates, and with the face's skin temperature dropping below 0°C, there is a significant risk of frostbite. Finally, extreme cold stress is identified by a core body temperature time gradient falling below -0.3 K/h and the rapid onset of freezing temperatures on the face, which indicates immediate danger (Błażejczyk et al. 2013).

Tab. 2 *UTCI equivalent temperatures categorized in terms of thermal stress and thermal perception.*

UTCI (°C)	Stress Category	Thermal Perception
> 46	Extreme heat stress	Torrid
38 ~ 46	Very strong heat stress	Hottish
32 ~ 38	Strong heat stress	Hot
26 ~ 32	Moderate heat stress	Warm
9 ~ 26	No thermal stress	Comfortable
0 ~ 9	Slight cold stress	Cool
-13 ~ 0	Moderate cold stress	Coolish
-27 ~ -13	Strong cold stress	Cold
-40 ~ -27	Very strong cold stress	Chilly
< -40	Extreme cold stress	Freezing

Studies have clearly documented a relationship between UTCI values and mortality rates. For instance, in Polish cities, an increase in resident mortality was observed on days when the UTCI exceeded 32°C, indicating strong heat stress

(Wieczorek et al. 2024). A specific case in June 2019 in Poland showed that deaths attributed to strong heat stress were five times higher than the average for the 2010–2018 reference period, with average noon UTCI values being 6.8°C higher. A significant pan-European study (Di Napoli et al. 2018) demonstrated UTCI's potential as a heat-related health risk indicator. This research, utilising 38 years of meteorological reanalysis data, found that the relationship between UTCI and death counts varies depending on the country's bioclimate. Generally, mortality increases under conditions of moderate (UTCI > 26°C) and strong (UTCI > 32°C) heat stress. UTCI's ability to represent mortality patterns was demonstrated during the 2003 European heatwave, where heat stress increased up to two UTCI categories above the seasonal average, leading to an excess number of deaths, particularly in Paris. In Paris, a strong correlation (r > 0.55) was found between UTCI and mortality, especially in the early morning and central daytime hours. In Bavaria, higher UTCI values in summer were consistently associated with an immediate (1–2 days) increase in daily mortality and hospital admissions, while a lagged (up to 14 days) decreasing effect of UTCI on mortality and hospital admissions was observed in the fall, winter and spring (Ghada et al. 2021).

Studies also note that while UTCI broadly reflects thermal stress, its representation for vulnerable groups, such as the elderly, might not be fully representative as the index is designed for an average healthy male person. Nevertheless, older individuals are particularly susceptible to heat/cold stress, thereby leading to higher hospital admissions and mortality in certain regions (Ghada et al. 2021; Urban et al. 2019).

Beyond mortality, UTCI has also been correlated with increased hospital admissions due to cardiovascular and respiratory diseases (Ghada et al. 2021), reduced outdoor labor productivity in sectors such as agriculture and construction (Črepinšek et al. 2023), higher winter road accident rates under cold stress (Ghada et al. 2021), and the decreased attractiveness of tourism when values exceed the comfort range of 9–26 °C (Wu et al. 2022). These findings emphasize the broader societal relevance of UTCI beyond its direct health impacts.

2 METHODS

This research utilizes a quantitative modeling approach to evaluate the anticipated effects of future climate change on human thermal comfort in Bratislava, Slovakia (48.2°N, 17.1°E). Bratislava was chosen as a representative example of a Central European urban climate that could be sensitive to future thermal stress. The approach is fundamentally based on the calculation and analysis of the UTCI.

Hourly weather data for a contemporary baseline period and for future projections (2040, 2060, 2080, and 2100) were generated using Meteonorm V8.0 software. Meteonorm is a globally recognized tool that produces reliable, site-specific climate data in the standard epw format by combining information from a comprehensive network of weather stations with satellite data and sophisticated interpolation algorithms. (Niknia and Ghiai 2025; Remund et al., 2023a)

The future climate projections were generated for three RCPs: RCP2.6, RCP4.5, and RCP8.5. The data for these scenarios within Meteonorm is derived from the IPCC AR5. Specifically, Meteonorm's calculations are based on a validated subset of 10 models from the Coupled Model Intercomparison Project, Phase 5 (CMIP5), which supply the full set of meteorological parameters needed for UTCI calculations, including temperature, humidity, wind components, and short and long-wave radiation. For intermediate future years, such as those used in this study, the software applies a linear interpolation between the standard future periods (e.g., 2011–2030, 2046–2065, and 2080–2099) as defined by the CMIP5 models (Remund et al., 2023b).

The epw weather files generated by Meteonorm were imported into the Grasshopper (Robert McNeel & Associates 2025) for processing. The calculation of the UTCI value for each hourly time step of the year was performed using components from the ClimateStudio V2.1 plugin (Solemma 2025). This process yielded a UTCI value for all 8,760 hours of the year for the contemporary baseline and for each of the future climate scenarios analyzed. The resulting data was then classified according to the established UTCI thermal stress categories for further analysis. The Grasshopper script used for evaluating the climate years is shown in Fig. 1.

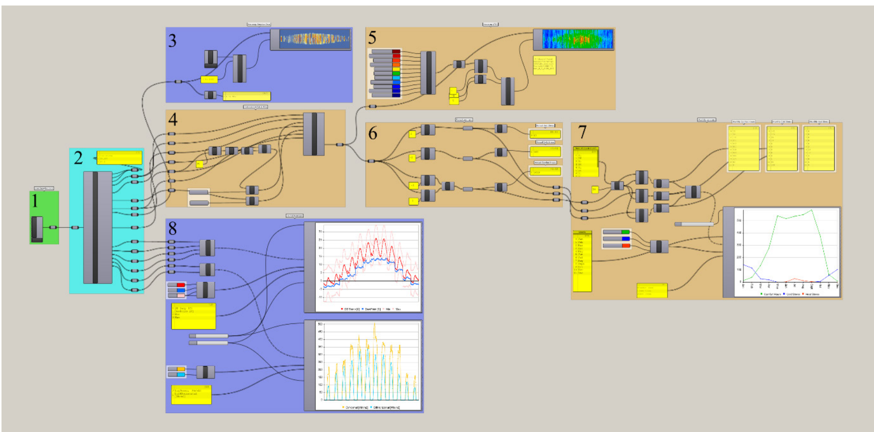

Fig. 1 *Grasshopper script used to analyse epw weather files: 1 - Loading the EPW file, 2 - Extracting Weather Data from the file, 3 - Visualization of Heatmap for Weather Data, 4 - UTCI calculations, 5 - Visualization of Heatmap for UTCI, 6 - Annual summary UTCI calculations, 7 - Monthly summary UTCI calculations, 8 - Diurnal Averages for temperature and solar radiation.*

The resulting UTCI data underwent a comprehensive statistical analysis to quantify the temporal trends and assess the significance of the projected changes. A linear regression analysis was performed on the annual heat and cold stress hours for each RCP scenario across the time series (2040, 2060, 2080, 2100) to determine the rates of change and the significance of any trends. The coefficient of determination (R^2) was calculated to assess the strength of the linear relationships, with the statistical significance evaluated at α=0.05. The descriptive statistics, including the means, standard deviations, and ranges, were computed for each scenario to characterize the central tendencies and their variability. The coefficient of variation (CV) was calculated as the ratio of the standard deviation to the mean and was expressed as a percentage to assess the relative variability within the scenarios and identify any increasing uncertainty under the higher emission pathways. The sizes of the effect were quantified by calculating changes in percentages from the contemporary baseline to evaluate the magnitude of the projected impacts. All the statistical analyses were performed using custom algorithms to ensure their reproducibility and accuracy. These algorithms, which were implemented in JavaScript, included the functions for linear regression (calculating the slope, intercept, and R^2 through the least-squares method), descriptive statistics (mean, standard deviation, coefficient of variation), and trend analysis across the temporal series (2040-2100). The custom implementation ensured full transparency in the mathematical operations and allowed for a tailored analysis specific to the UTCI dataset structure. The temporal trends were tested for statistical significance using t-statistics with n-2 degrees of freedom, where n represents the number of time points. This multi-faceted statistical approach provided robust quantitative evidence for evaluating the hypotheses regarding any future bioclimatic changes in Bratislava.

3 RESULTS

The analysis of the climate data generated for the contemporary period and future scenarios is presented through a series of heatmaps (Figs. 2 and 3) and graphs (Figs. 4 to 6). These visualizations illustrate the projected changes in temperature and UTCI-derived thermal stress categories for Bratislava. The statistical analysis reveals significant temporal trends and scenario-dependent variations in thermal stress patterns. The dry bulb temperature was selected for the heatmaps as it represents the most direct and widely understood measure of ambient air conditions. The annual distribution of the dry bulb temperature is shown in Fig. 2. The contemporary heatmap displays a distinct seasonal cycle, with cold conditions in the winter and warm-to-hot conditions concentrated in the summer months. In the future projections, all the scenarios show a progressive increase in temperatures. The effect is most pronounced under the RCP8.5 scenario, which exhibits a significant expansion and intensification of hot periods by the end of the century.

Fig. 3 translates these changes in temperature into UTCI thermal stress categories. The contemporary period is characterized by prevalent "no" thermal stress conditions (green), with significant periods of cold stress (blue) in the winter, and instances of heat stress (yellow to red) during summer afternoons. For the future scenarios, the heatmaps show a clear trend, i.e., a reduction in the duration and intensity of the cold stress and a marked increase in the frequency and severity of the heat stress. By 2100, the RCP8.5 scenario indicates that "Strong" and "Very strong" heat stress will become common during the summer months.

The monthly distribution of the hours under strong heat stress (UTCI ≥ +32°C) is detailed in Fig 4. In the contemporary baseline, such conditions are infrequent and limited to June, July, and August; a total of only 66 annual hours. All the future scenarios project an increase in these hours, which start earlier in the year and extend later. The linear regression analysis demonstrates strong positive trends: RCP2.6 shows a minimal change (slope = -0.35 hours/year, R^2 = 0.125), RCP4.5 exhibits a moderate increase (+2.26 hours/year, R^2 = 0.978, $p < 0.05$), while RCP8.5 displays dramatic acceleration (+12.23 hours/year, R^2 = 0.975, $p < 0.05$). The increase is most dramatic in the RCP8.5 scenario, which projects over 350 hours of strongheat stress in July alone by 2100.

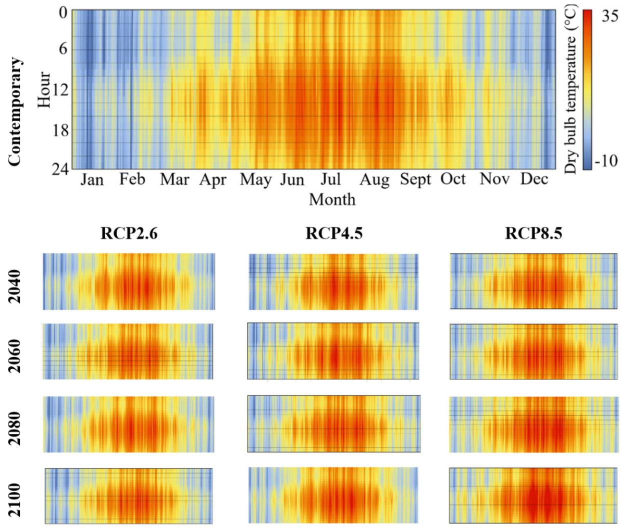

Fig. 2 *Dry bulb temperature heatmaps - contemporary period and future projections (generated using Grasshopper for Rhino).*

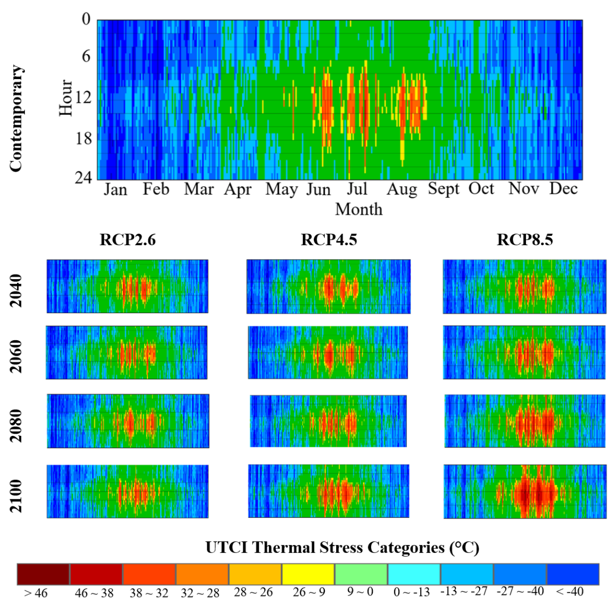

Fig. 3 *UTCI Heatmaps - contemporary period and future projections (generated using Grasshopper for Rhino).*

Fig. 5 shows the projected changes in the comfort hours (+9°C ≤ UTCI ≤ +26°C). The contemporary data shows peaks in the comfortable hours during May and September. Future projections indicate a decrease in the comfort hours during the summer months (June-August) as temperatures shift into heat stress categories. This reduction is most significant under RCP8.5, particularly by the years 2080 and 2100.

The analysis of the cold stress hours (UTCI ≤ 0°C) presented in Fig. 6, reveals a consistent decline across all the scenarios and future periods. The statistical analysis confirms significant negative trends: RCP2.6 (-1.42 hours/year, R^2 = 0.104), RCP4.5 (-3.51 hours/year, R^2 = 0.626), and RCP8.5 (-3.98 hours/year, R^2 = 0.735). While the cold stress is common in the contemporary winter months, its frequency diminishes significantly in all the projections, with the most substantial reduction being observed in the RCP8.5 scenario.

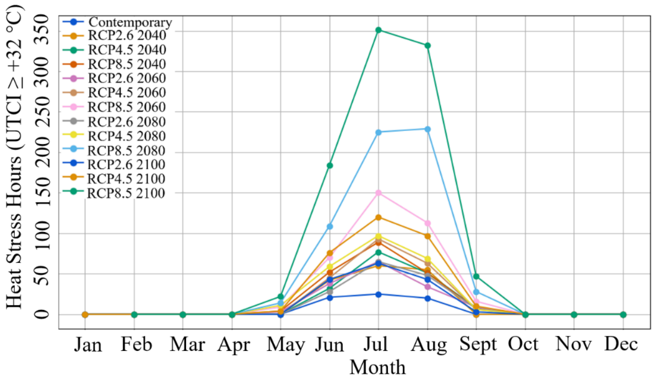

Fig. 4 *Monthly Heat Stress Hours - contemporary period and future projections.*

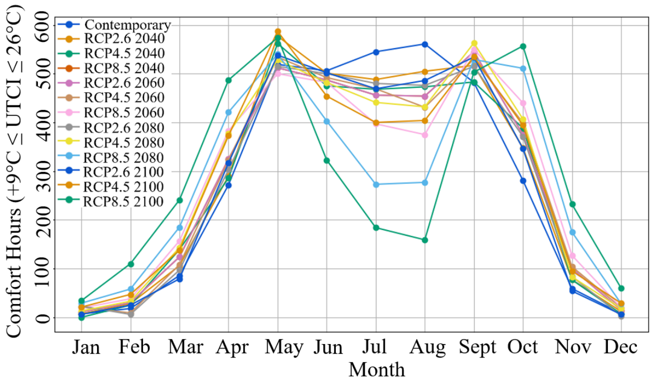

Fig. 5 *Monthly Comfort Hours- contemporary period and future projections*

The cumulative annual data summarizes these trends. Fig. 7 illustrates the total annual hours of strong heat stress. The contemporary period baseline is 66 hours. By 2100, this is projected to increase to 152 hours under RCP2.6 (+130%), 307 hours under RCP4.5 (+365%), and 936 hours under RCP8.5 (+1,318%). Finally, Fig. 8 shows the total annual hours of cold stress. Starting from approximately 851 hours in the contemporary period, the number of cold stress hours is projected to decrease across all the scenarios. By 2100, the cold stress hours will have been reduced to 688 under RCP2.6 (-19%), 519 under RCP4.5 (-39%), and 312 hours under RCP8.5 (-63%).

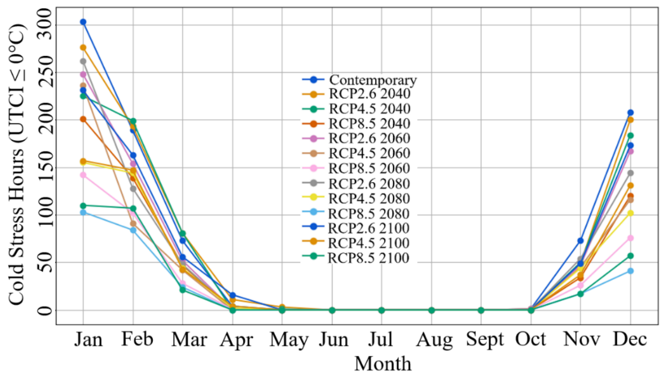

Fig. 6 *Monthly Cold Stress Hours - contemporary period and future projections.*

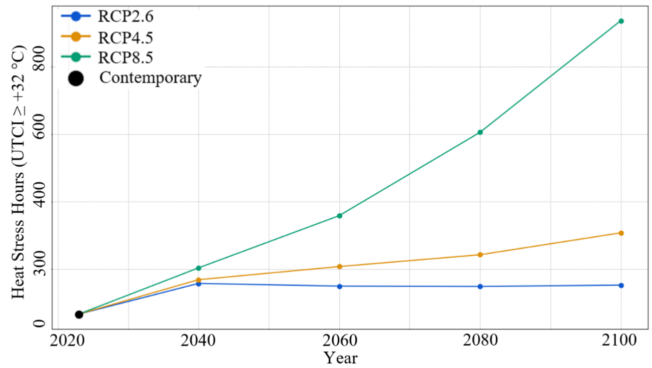

Fig. 7 *Annual Heat Stress Hours - contemporary period and future projections.*

The coefficient of variation analysis reveals increasing uncertainty concerning the intensity of emissions: RCP2.6 shows low variability (CV=16% for heat, 17% for cold), RCP4.5 moderate variability (CV=26% for heat, 20% for cold), and RCP8.5 high variability (CV=61% for heat, 32% for cold), which indicate greater unpredictability in extreme scenarios.

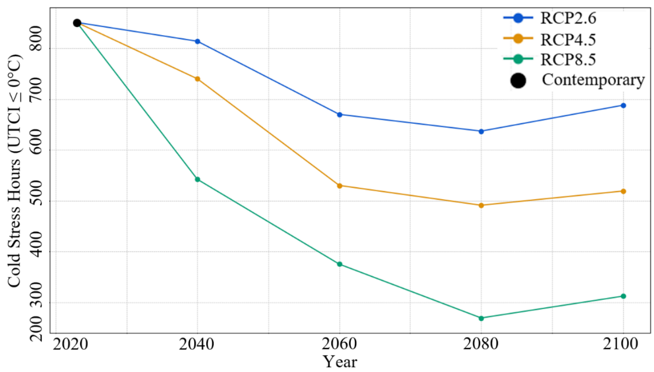

Fig. 8 *Annual Cold Stress Hours - contemporary period and future projections.*

4 DISCUSSION

The results of this study clearly demonstrate a significant projected transformation of Bratislava's bioclimatic environment throughout the 21st century, with the severity of the change being highly dependent on the RCP. The statistical analysis confirms these changes are not random variations but robust temporal trends. The high coefficient of determination ($R^2 > 0.97$ for RCP4.5 and RCP8.5) indicates that the projected changes correlate very strongly with time within these scenarios. The primary finding is a dual-fronted shift, i.e., a dramatic increase in the frequency and intensity of summer heat stress coupled with a substantial decrease in winter cold stress.

The most striking outcome is the projected surge in hours of the strong heat stress (UTCI ≥ +32°C), particularly under the high-emissions RCP8.5 scenario, where annual hours of strong heat stress may increase 14.2-fold from a baseline of 66 to 936 hours. The linear regression analysis reveals an acceleration rate of 12.23 hours per year ($R^2 = 0.975$, $p < 0.05$), which indicates that this is not a gradual change but an exponential transformation. This finding moves beyond a simple observation of rising average temperatures; it quantifies the impact on human physiological experience. By beginning earlier in the spring and extending into autumn, the expansion of the heat stress season suggests that periods of dangerously hot weather will become a more common and prolonged feature of life in Bratislava.

This has profound public health implications. Studies in nearby European regions have established a direct link between UTCI values exceeding +32°C and increased mortality rates (Di Napoli et al. 2018; Wieczorek et al. 2024; Ghada et al. 2021). As previously noted, prolonged periods of strong heat stress are closely associated with excess deaths, and the projected increase in such conditions for Bratislava signals a substantial future health challenge not only for local authorities but also for public health systems and urban planners. Therefore, the projected increase in such conditions for Bratislava signals a substantial future public health challenge, which may likely lead to a higher incidence of heat-related morbidity and mortality, especially among vulnerable populations such as the elderly.

Concurrently, the sharp decline in annual cold stress hours (UTCI ≤ 0°C) across all the scenarios represents a fundamental shift in the character of Bratislava's winters. The statistical analysis confirms significant negative trends, with RCP8.5 showing a reduction rate of 3.98 hours per year (R^2=0.735). The number of cold stress hours is projected to fall from 851 in the contemporary period to 312 by 2100 under RCP8.5, a 63% reduction. On the one hand, this may yield certain benefits. For example, some studies have associated increases in winter UTCI with immediate decreases in daily road accidents (Ghada et al. 2021). Furthermore, as cold weather is linked to an increase in injury rates in outdoor occupations, including slipping, tripping, and falling accidents, milder conditions could reduce these risks (Holmér et al. 2012).

The analysis of comfort hours reveals that while winter may become less harsh, summer could become increasingly uncomfortable, which would lead to a net decrease in comfortable hours, especially from June to August. The high coefficient of variation in RCP8.5 (CV=61% for heat stress) indicates increasing unpredictability and suggests that extreme events may become more variable and harder to predict. The city's climate is projected to transition from one with distinct, manageable seasons to one with prolonged, stressful summers and milder, shorter winters. This shift has consequences for tourism, lifestyles, outdoor labor productivity, and the city's overall sense of place.

Limitations of the Study

The use of UTCI provides a more complete picture of environmental stress than an analysis of temperature alone. However, the application of this standardized index has inherent limitations. The UTCI Index is calculated based on the thermophysiological response of an average, healthy 35-year-old male walking at a set speed (Bröde et al. 2013). As noted in the literature, this may not fully represent the thermal perception and vulnerability of other demographics, particularly the elderly, children, or individuals with pre-existing health conditions who are more susceptible to thermal stress (Urban et al. 2019).

The climate data generated by Meteonorm represents a 'regional baseline' for the general climate of the Bratislava region (48.2°N, 17.1°E), not a specific intra-urban location. It does not account for localized microclimatic variations within the city, most notably the urban heat island (UHI) effect. Therefore, the actual heat stress experienced by residents in densely built-up, unshaded parts of Bratislava could be even higher than our regional projections indicate. Furthermore, the UTCI calculations rely on the modeled radiation data (short- and long-wave) generated by Meteonorm, which is based on CMIP5 models. While this is a standard approach for future climate projections, this modeled radiation data carries its own uncertainties, which are propagated into the final UTCI values. Similarly, projections of relative humidity from global climate models (GCMs) are a known source of uncertainty (Chakraborty et al. 2022). As relative humidity is a critical input for the UTCI, any inaccuracies in its future projection will directly impact the thermal stress calculations presented in this study.

Future Research

This research serves as a robust climatological projection. The next scientific step should be to move toward a fully integrated risk assessment. This would involve coupling these bioclimatic models with detailed demographic data, urban morphology maps, and public health statistics. Such an approach would allow for the creation of dynamic risk maps for Bratislava and would identify which populations and which parts of the city are most vulnerable. A key step in this process would be to integrate locally measured climate data, as the importance of site-specific measurements for capturing unique urban conditions has been demonstrated in other Slovak cities (Juras and Jurasova 2020). By bridging the gap between large-scale climate modeling and local-scale impact, future research could provide the actionable intelligence needed for effective climate adaptation. Such insights are highly relevant for building engineers, as they can inform the design of resilient buildings, infrastructures, and urban environments that safeguard human health under future climatic conditions.

5 CONCLUSION

Like many other cities worldwide, Bratislava will not remain an exception and will be challenged by the profound impacts of a changing climate. This study's analysis unequivocally shows that Bratislava faces a significant bioclimatic transformation by the end of the 21st century, with the severity of the change directly linked to future greenhouse gas emission pathways. The central hypothesis, i.e., that climate change would fundamentally alter the city's thermal character, was confirmed through robust statistical analysis demonstrating strong temporal trends ($R^2 > 0.97$) and significant scenario-dependent variations.

The key quantitative findings include:

- heat stress hours could increase from 66 to as high as 936 by 2100 under RCP8.5, following a strongly linear trend (+12.23 hours/year),
- cold stress hours could decrease from 851 to as low as 312, which would be a 63% reduction,
- the coefficient of variation could increase with the intensity of emissions and reach 61% for RCP8.5 heat stress, thereby indicating growing uncertainty in extreme scenarios.

This research contributes a crucial, localized dataset to a broader understanding of climate change impacts in Central Europe. By translating abstract global emissions pathways into tangible, human-centric metrics for Bratislava, which are supported by rigorous statistical validation, this work provides a vital evidence base for local policymakers, urban planners, and public health officials. The clear divergence between the outcomes of the RCP scenarios underscores the profound impact of global climate policy on the future livability of the city and provides the actionable intelligence needed to inform and motivate robust climate adaptation strategies. In this context, climate change will also require a new approach to building design, with a greater use of advanced materials and modern technologies to ensure good indoor environments and maintain comfortable microclimates within buildings.

6 ACKNOWLEDGEMENT

This research was supported by the Young STU Researchers Support Programme under Grant No. 1634, the Slovak Research and Development Agency (APVV) under Grant No. 18-0174 and the Cultural and Educational Grant Agency of the Ministry of Education, Science, Research and Sport of the Slovak Republic (KEGA) under Grant No. 036STU-4/2025.

REFERENCES

BJØRNÆS, Christian (2022). *A guide to Representative Concentration Pathways.* Online. CICERO. Available at: https://cicero.oslo.no/en/articles/a-guide-to-representative-concentration-pathways.

BŁAŻEJCZYK, Krzysztof; Gerd JENDRITZKY; Peter BRÖDE; Dusan FIALA; George HAVENITH; Yoram EPSTEIN; Agnieszka PSIKUTA and Bernhard KAMPMANN (2013). *An introduction to the Universal Thermal Climate Index (UTCI).* Online. Geographia Polonica, vol. 86, No. 1, pp. 5–10. ISSN 00167282. Available at: https://doi.org/10.7163/GPol.2013.1.

BRÖDE, Peter; Krzysztof BLAZEJCZYK; Dusan FIALA; George HAVENITH; Ingvar HOLMÉR; Gerd JENDRITZKY; Kalev KUKLANE and Bernhard KAMPMANN (2013). *The Universal Thermal Climate Index UTCI Compared to Ergonomics Standards for Assessing the Thermal Environment. Online. Industrial Health,* vol. 51, No. 1, pp. 16–24. ISSN 0019-8366, 1880-8026. Available at: https://doi.org/10.2486/indhealth.2012-0098.

BRÖDE, Peter; Dusan FIALA; Krzysztof BŁAŻEJCZYK; Ingvar HOLMÉR; Gerd JENDRITZKY; Bernhard KAMPMANN; Birger TINZ and George HAVENITH (2012). *Deriving the operational procedure for the Universal Thermal Climate Index (UTCI).* Online. International Journal of Biometeorology, vol. 56, No. 3, pp. 481–494. ISSN 0020-7128, 1432-1254. Available at: https://doi.org/10.1007/s00484-011-0454-1.

BRÖDE, Peter; Gerd JENDRITZKY; Dusan FIALA and George HAVENITH (2010). *The Universal Thermal Climate Index UTCI in Operational Use.* Online. In: Proceedings of Adapting to Change: New Thinking on Comfort. London: Network for Comfort and Energy Use in Buildings. Available at: http://nceub.org.uk.

BRÖDE, Peter; Eduardo L KRÜGER and Francine A ROSSI (2011). *Assessment of urban outdoor thermal comfort by the Universal Thermal Climate Index (UTCI).* Online. In: Proceedings of the 14th International Conference on Environmental Ergonomics., pp. 338–341. Available at: https://www.researchgate.net/publication/322991510.

CHAKRABORTY, T.; Z. S. VENTER; Y. QIAN and X. LEE (2022). *Lower urban humidity moderates outdoor heat stress.* Online. AGU Advances, vol. 3, p. e2022AV000729. Available at: https://doi.org/10.1029/2022AV000729.

ČREPINŠEK, Zalika; Zala ŽNIDARŠIČ and Tjaša POGAČAR (2023). *Spatio-Temporal Analysis of the Universal Thermal Climate Index (UTCI) for the Summertime in the Period 2000–2021 in Slovenia: The Implication of Heat Stress for Agricultural Workers.* Online. Agronomy, vol. 13, No. 2, p. 331. ISSN 2073-4395. Available at: https://doi.org/10.3390/agronomy13020331.

DI NAPOLI, Claudia; Florian PAPPENBERGER and Hannah L. CLOKE (2018). *Assessing heat-related health risk in Europe via the Universal Thermal Climate Index (UTCI).* Online. International Journal of Biometeorology, vol. 62, No. 7, pp. 1155–1165. ISSN 0020-7128, 1432-1254. Available at: https://doi.org/10.1007/s00484-018-1518-2.

GHADA, Wael; Nicole ESTRELLA; Donna P. ANKERST and Annette MENZEL (2021). *Universal thermal climate index associations with mortality, hospital admissions, and road accidents in Bavaria.* Online. PLOS ONE, vol. 16, No. 11, p. e0259086. ISSN 1932-6203. Available at: https://doi.org/10.1371/journal.pone.0259086.

HOLMÉR, Ingvar; Juhani HASSI; Tiina M. IKÄHEIMO and Jouni J. K. JAAKKOLA (2012). *Cold Stress: Effects on Performance and Health.* Online. In: Eula BINGHAM, Barbara COHRSSEN and Charles H. POWELL (eds.). Patty's Toxicology. 1st ed. Wiley, pp. 1–26. ISBN 978-0-471-31943-6. Available at: https://doi.org/10.1002/0471435139.tox097.pub2.

INTERGOVERNMENTAL PANEL ON CLIMATE CHANGE (2014). *The IPCC's Fifth Assessment Report (AR5).* Online. IPCC. Available at: https://www.ipcc.ch.

JURAS, Peter and Daniela JURASOVA (2020). *Outdoor climate change analysis in university campus: Case study with heat-air-moisture simulation.* Online. Civil and Environmental Engineering, vol. 16, No. 2, pp. 370-378. Available at: https://doi.org/10.2478/cee-2020-0037.

JENDRITZKY, Gerd; Abdel MAAROUF; Dusan FIALA and Henning STAIGER (2002). *An update on the development of a Universal Thermal Climate Index.* In: Proceedings of the 15th Conference on Biometeorology and Aerobiology and 16th International Congress of Biometeorology, vol. 27. Kansas City: AMS, pp. 129-133. Available at: https://ams.confex.com/ams/15BioAero/techprogram/paper_49599.htm.

MEINSHAUSEN, Malte; S. J. SMITH; K. CALVIN; J. S. DANIEL; M. L. T. KAINUMA; J-F. LAMARQUE; K. MATSUMOTO; S. A. MONTZKA; S. C. B. RAPER; K. RIAHI; A. THOMSON; G. J. M. VELDERS and D.P. P. VAN VUUREN (2011). *The RCP greenhouse gas concentrations and their extensions from 1765 to 2300.* Online. Climatic Change, vol. 109, Nos. 1–2, pp. 213–241. ISSN 0165-0009, 1573-1480. Available at: https://doi.org/10.1007/s10584-011-0156-z.

MOSS, Richard H.; Jae A. EDMONDS; Kathy A. HIBBARD; Martin R. MANNING; Steven K. ROSE; Detlef P. VAN VUUREN; Timothy R. CARTER; Seita EMORI; Mikiko KAINUMA; Tom KRAM; Gerald A. MEEHL; John F. B. MITCHELL; Nebojsa NAKICENOVIC; Keywan RIAHI; Steven J. SMITH; Ronald J. STOUFFER; Allison M. THOMSON; John P. WEYANT and Thomas J. WILBANKS (2010). *The next generation of scenarios for climate change research and assessment.* Online. Nature, vol. 463, No. 7282, pp. 747–756. ISSN 0028-0836, 1476-4687. Available at: https://doi.org/10.1038/nature08823.

NASSIRI, Parvin; Mohammad Reza MONAZZAM; Farideh GOLBABAEI; Somayeh Farhang DEHGHAN; Athena RAFIEEPOUR; Ali Reza MORTEZAPOUR and Mehdi ASGHARI (2017). *Application of Universal Thermal Climate Index (UTCI) for assessment of occupational heat stress in open-pit mines.* Online. INDUSTRIAL HEALTH, vol. 55, No. 5, pp. 437–443. ISSN 0019-8366, 1880-8026. Available at: https://doi.org/10.2486/indhealth.2017-0018.

NIKNIA, Sepideh and Mehdi GHIAI (2025). *Simulation-Based Prediction of Office Buildings Energy Performance Under RCP Scenarios Across All U.S. Climate Zones.* Online. Architecture, vol. 5, No. 2, p. 34. ISSN 2673-8945. Available at: https://doi.org/10.3390/architecture5020034.

REFERENCES

PECELJ, Milica M.; Milica Z. LUKIĆ; Dejan J. FILIPOVIĆ; Branko M. PROTIĆ and Uroš M. BOGDANOVIĆ (2020). *Analysis of the Universal Thermal Climate Index during heat waves in Serbia.* Online. Natural Hazards and Earth System Sciences, vol. 20, No. 7, pp. 2021–2036. ISSN 1684-9981. Available at: https://doi.org/10.5194/nhess-20-2021-2020.

REMUND, Jan; Stefan MÜLLER; Michael SCHMUTZ; Daniele BARSOTTI; Pascal GRAF and René CATTIN (2023a). *Meteonorm 8, Handbook part I: Software.* Online. Meteotest AG. Available at: https://www.meteonorm.com/en/downloads.

REMUND, Jan; Stefan MÜLLER; Michael SCHMUTZ; Daniele BARSOTTI; Pascal GRAF and René CATTIN (2023b). *Meteonorm 8, Handbook part II: Theory.* Online. Meteotest AG. Available at: https://www.meteonorm.com/en/downloads.

ROBERT MCNEEL & ASSOCIATES (2025). *Grasshopper: Algorithmic modeling for Rhino.* Online. Available at: https://www.grasshopper3d.com

SOLEMMA (2025). *ClimateStudio: Environmental Performance Analysis for Buildings.* Online. Solemma, LLC. Available at: https://www.solemma.com

URBAN, Aleš; David M. HONDULA; Hana HANZLÍKOVÁ and Jan KYSELÝ (2019). *The predictability of heat-related mortality in Prague, Czech Republic, during summer 2015—a comparison of selected thermal indices.* Online. International Journal of Biometeorology, vol. 63, No. 4, pp. 535–548. ISSN 0020-7128, 1432-1254. Available at: https://doi.org/10.1007/s00484-019-01684-3.

VAN VUUREN, Detlef P.; Jae EDMONDS; Mikiko KAINUMA; Keywan RIAHI; Allison THOMSON; Kathy HIBBARD; George C. HURTT; Tom KRAM; Volker KREY; Jean-Francois LAMARQUE; Toshihiko MASUI; Malte MEINSHAUSEN; Nebojsa NAKICENOVIC; Steven J. SMITH and Steven K. ROSE (2011). *The representative concentration pathways: an overview.* Online. Climatic Change, vol. 109, Nos. 1–2, pp. 5–31. ISSN 0165-0009, 1573-1480. Available at: https://doi.orgorg/10.1007/s10584-011-0148-z.

WAYNE, Graham (2013). *The Beginner's Guide to Representative Concentration Pathways.* Online. Skeptical Science. Available at: https://skepticalscience.com/rcp.php.

WIECZOREK, Joanna; Bogdan BOCHENEK; Tomasz STRZYŻEWSKI; Monika HAJTO; Piotr SEKUŁA; Anita BOKWA and Mirosław ZIMNOCH (2024). *Daily heat stress in Kraków in the warm period 2012–2022 based on hourly meteorological measurements and radiative fluxes derived from satellite systems.* Online. Acta Geographica Lodziensia, vol. 117. ISSN 00651249, 24510319. Available at: https://doi.org/10.26485/AGL/2024/117/9.

WU, Jinkui; Tian JIN; Yancong WU; Yongjian DING; Yaqiong MU and Di ZENG (2022). T*he Variation of UTCI with the Background of Climate Change and Its Implications for Tourism in a Complicated Climate Region in Western China.* Online. Sustainability, vol. 14, No. 22, p. 15047. ISSN 2071-1050. Available at: https://doi.org/10.3390/su142215047.

ZHAI, Z. J. and J. M. HELMAN (2019). *Climate change: Projections and implications to building energy use.* Online. Building Simulation, vol. 12, No. 10, pp. 585–596. ISSN 1996-3599, 1996-8744. Available at: https://doi.org/10.1007/s12273-019-0509-5.